JOURNAL OF APPLIED ELECTROCHEMISTRY 19 (1989) 43–50

Flow-through and flow-by porous electrodes of nickel foam. I. Material characterization

S. LANGLOIS, F. COEURET

Laboratoire de Génie des Procédés, CNRS, Ecole Nationale Supérieure de Chimie de Rennes, Avenue du Général Leclerc, 35700 Rennes-Beaulieu, France

Received 21 October 1987; revised 15 July 1988

This paper deals with the characterization of three nickel foams for use as materials for flow-through or flow-by porous electrodes. Optical and scanning electron microscope observations were used to examine the pore size distribution. The overall, apparent electrical resistivity of the reticulated skeleton was measured. The BET method and the liquid permeametry method were used to determine the specific surface area, the values of which are compared with those known for other materials.

Nomenclature

a_e	specific surface area (per unit of total volume) (m^{-1})
a_s	specific surface area (per unit of solid volume) (m^{-1})
$(a_e)_{BET}$	specific surface area determined by the BET method (m^{-1})
$(a_e)_{Ergun}$	specific surface area determined by pressure drop measurements (m^{-1})
$\bar{d}_p$	mean pore diameter (m)
$(\bar{d}_p)_{micro}$	mean pore diameter determined by optical microscopy (m)
$(\bar{d}_p)_{Ergun}$	mean pore diameter using Ergun equation (m)
e	thickness of the skeleton element of the foam (m)
G	grade of the foam (number of pores per inch)
$\Delta P/H$	pressure drop per unit height of the foam ($Pa\,m^{-1}$)
r	electrical resistivity ($\Omega\,m$)
R_h	hydraulic pore radius (m)
T	tortuosity
$\bar{u}$	mean liquid velocity ($m\,s^{-1}$)

Greek symbols

$\bar{\varepsilon}$	mean porosity
γ	circularity factor
μ	dynamic viscosity ($kg\,m^{-1}\,s^{-1}$)
ϱ	liquid density ($kg\,m^{-3}$)
σ	pore diameter size dispersion

1. Introduction

Among the numerous porous materials available for flow-through and flow-by porous electrodes, reticulated structures are novel. Copper foams were made by Tentorio *et al.* [1] by chemical copper deposition on polyurethane foams followed by electrochemical copper deposition; they were tested as cathodes for electrolytic copper recovery. Nickel foam electrodes were used by Cox [2] and some of his results were considered again in [3, 4]. More recently, a copper foam electrode was used in electroorganic synthesis [5], while reticulated vitreous carbon or RVC began to be commercially available [6] and started to be applied, at least on laboratory scale, to remove, for example, mercury from contaminated brine solutions [7]. Nickel foams, which also have a reticulated texture, are now industrially produced and are available for electrolytic use. These are produced by SORAPEC [8]. A previous appraisal of the performance of flow-through porous electrodes made of nickel foam was made by the authors [9]; the main aim was to determine the magnitude of the limiting diffusion currents at these electrodes. Unfortunately, the materials used in [9] were not geometrically characterized; their specific surface areas were approached by the BET method and were found to be around $130\,000\,m^{-1}$, a value significantly higher than the true electrochemical active area. A more general study of the application of the foam as three-dimensional electrodes was necessary. The manufacturer characterizes a foam texture by the value of the 'grade' which designates the number of pores present in the structure per inch (or ppi); thus 'grade' and 'ppi' are identical denominations. It was decided to restrict the study to three nickel foams of grade 45, 60 and 100. These are designated below by G45, G60 and G100, respectively.

The present paper deals with the geometrical characterization of these three nickel foams. In a second part [10], mass transfer to porous electrodes made of these foams is discussed, while a third part [11] will concern, more specifically, the potential distribution within electrodes having a geometry suitable to industrial application.

Before considering the application of the foams as porous electrodes percolated by the electrolyte in

0021-891X/89 $03.00 + .12

forced flow (flow-through or flow-by porous electrodes), some parameters must be known, e.g.: (a) geometrical properties such as porosity, specific surface area, pore diameter distribution, isotropy of the texture, tortuosity, surface state, etc.; (b) physical properties such as hydraulic diameter, permeability, electrical conductivity, mechanical strength, etc.

The results given in the present paper concern these various parameters

2. Microscopic observations of the foams

The nickel foams studied are commercially manufactured in the form of rectangular sheets 0.0025 m thick. X-ray spectroscopy indicates that the surface is pure nickel.

2.1. *Qualitative results*

The observation of the three foams using a binocular, optical microscope reveals that they have similar aspect and structure. They appear as very porous media with alveolar-type pores; the various small alveoli are interconnected so that the overall texture looks like a juxtaposition of polygonal cavities. Their texture is similar to that of vitreous carbon foams (RVC).

The photographs of Fig. 1 correspond to the foam G100; they were obtained by scanning electron microscopy, with a magnification varying between 30 and 6000. Figures 1a and 1b clearly show that the unit element is a polygonal skeleton defining an alveolus; it is also clear that the pore size (the pores are the alveoli and also the openings between neighbouring alveoli) is dispersed.

Figure 1c presents a side or blade of the skeleton and its junction at a node with three other elements. Figure 2 shows the sectioned area of one element; it can be seen that this section is triangular with round extremities; its thickness is nearly constant except at the immediate vicinity of a node. At the higher magnification (Fig. 1d) it is clear that the surface is a mosaic. The electron microscopy does not

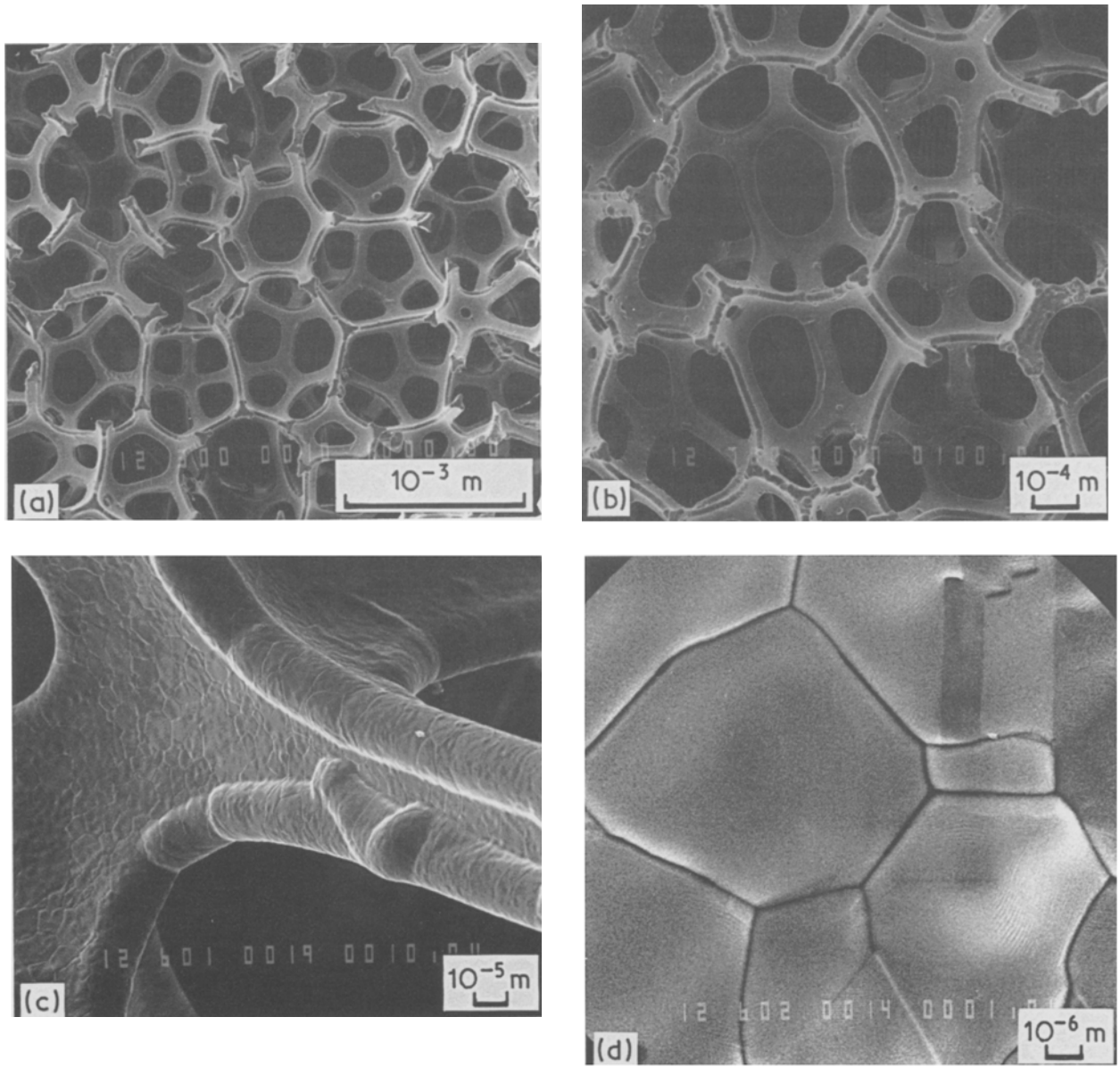

Fig. 1. Photographs of the foam G100 at various magnifications: (a) × 30; (b) × 78; (c) × 600; (d) × 6000.

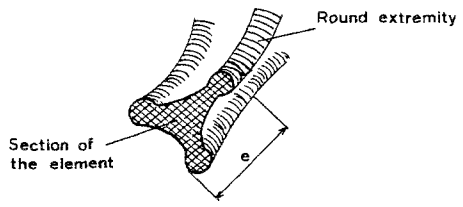

Fig. 2. Schematic representation of a sectioned element of a foam.

reveal significant microporosity in the solid elements. elements.

2.2. *Pore size distribution*

The pore size distribution was deduced from optical microscopy; the pores considered on a given photograph are those located in the definition plane of the picture. The cross sectional area, S, of each observed pore is approximated to that of a circle of diameter d_p. A population of more than 50 samples is considered for each foam, but the pores examined are principally the interalveolar pores. The uncertainty (about 10%) on the value of d_p is due to the inclination of the plane of the pore opening from the plane of the photograph.

Figure 3 shows, as an example, a histogram of the pore diameter distribution for the foam G60; several peaks which reveal the combination of neighbouring underpopulations, are present. Table 1 gives the values obtained for the mean diameter $\bar{d}_p$ of the equivalent circle, the standard deviation around the mean diameter, the relative deviation $\sigma/\bar{d}_p$, the ratio $\bar{d}_{p100}/\bar{d}_{p_i}$ which compares the $\bar{d}_p$ value of the foam G100 to those of a foam G_i, and the thickness e of the skeleton element far from a node.

The uniformity of the distribution decreases from the foam G100 to the foam G45, but the relative dispersion $\sigma/\bar{d}_p$ is nearly the same and equal to 0.25 for the three foams. This constancy of $\sigma/\bar{d}_p$ establishes the similarity of the three materials studied and, according to [12], provides for the determinant influence of the specific surface area on the performance of the three foams when they operate in a pure laminar flow regime. Indeed, it was shown [12, 13] that the uniformity of the pore size distribution of a three-dimensional electrode greatly influences the electrode behaviour, in comparison with the influence of the specific surface area.

Table 1. Characteristic dimensions deduced for the foams by optical microscopy

	Foam		
	G100	*G60*	*G45*
$(\bar{d}_p)_{micro}$ (m)	2×10^{-4}	3×10^{-4}	4.4×10^{-4}
σ (m)	5×10^{-5}	6.5×10^{-5}	10^{-4}
$\sigma/(\bar{d}_p)_{micro}$	0.25	0.22	0.23
$\bar{d}_{100}/\bar{d}_i$	1	0.66	0.45
e (m)	5.5×10^{-5}	7.5×10^{-5}	1.1×10^{-4}
$e/(\bar{d}_p)_{micro}$	0.27	0.25	0.25

It can be deduced from Table 1 that

$$(\text{grade})_{\text{foam i}} = 100 \frac{\bar{d}_{p100}}{\bar{d}_{p_i}} \qquad (1)$$

and that the thickness, e, is approximately equal to $0.25\bar{d}_p$ for each foam.

As a conclusion these measurements, using an optical microscope, allowed the determination of $(\bar{d}_p)_{micro}$ and established the similarity of the structure of the three foams.

3. Determination of other characteristics

Table 2 summarizes results of different measurements made on the three foams; for comparison data

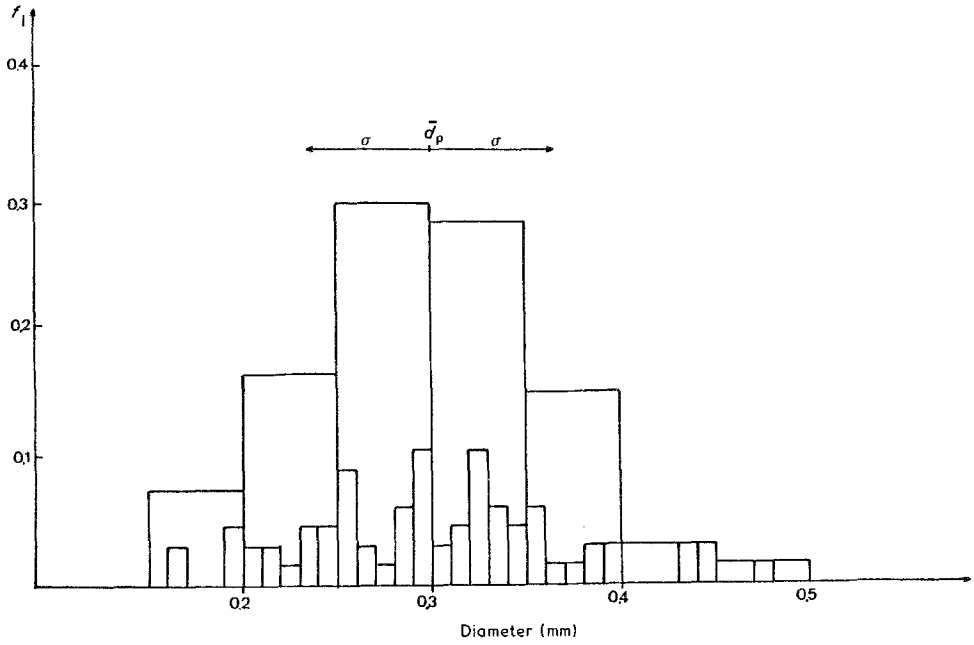

Fig. 3. Distribution of the pore diameter in foam G60. $\bar{d}_p = 0.300$ mm, $\sigma = 0.065$ mm, $N = 68$.

Table 2. Results of measurements made on the foams and comparison with the foam RVC

	Foam			
	G100	*G60*	*G45*	*RVC 100 ppi* [14]
Sheet thickness (m)	2.1×10^{-3}	2.55×10^{-3}	2.7×10^{-3}	-
Density ($kg\,m^{-3}$)	~250	~235	~230	~48
Mean porosity ($\bar{\varepsilon}$)	0.973	0.975	0.978	0.97
Apparent electrical resistivity (r_{foam})	1.04×10^{-5}* 1.32×10^{-5}†	1.10×10^{-5}* 1.34×10^{-5}†	1.12×10^{-5}* 1.46×10^{-5}†	4.7×10^{-3}–6.9×10^{-3} at 25°C

† Measurements made in the direction perpendicular to case *.

previously published for 100 ppi reticulated vitreous carbon (RVC) [14] are included in this table.

The overall mean porosity of the foams is about 0.975, a value which is the same as for the 100 ppi RVC. The porosity is found by weighing a known volume of the foam, which would consist of pure nickel. The apparent overall density is about $250\,kg\,m^{-3}$, a value 5 times higher than for RVC.

However, the nickel foam – and it is also true for other metals – does not suffer the fragility of the RVC and it is easier to feed the electrical current to the former than to the latter. A great advantage of the nickel foam is its low electrical resistivity. The apparent electrical resistivity, r_{foam}, of each foam was deduced from the slope of experimental current–voltage lines; the measurements applied d.c. currents (with intensity up to 50 A) to rectangular samples of foam with air ventilation at constant (35°C) temperature. In the experimental conditions used, the electrical conduction in the foams obeyed Ohm's law. Also the apparent electrical resistivity was measured in two perpendicular directions of the general current flow. The values given in Table 2 show: (i) that the three foams have approximately the same electrical resistivity, the value of which is between 10^{-5} and $1.5 \times 10^{-5}\,\Omega m$. As the nickel electrical resistivity r_{Ni} at 35°C is $7.5 \times 10^{-8}\,\Omega m$, r_{foam} can be expressed in the following manner:

$$r_{foam} \approx \frac{4}{(1 - \bar{\varepsilon})} r_{Ni} \qquad (2)$$

(ii) the values of r_{foam} deduced from measurements in two perpendicular directions differ by a factor of 1.25. This reveals some anisotropy of the texture.

4. Specific surface area

Generally, it is not easy to know the true electrochemically active specific surface area of porous materials [15, 16] and the values obtained for a given material seem to depend on the method used [15, 17]. Otherwise various definitions of specific surface area can be given. Generally mass balances use the specific surface area per unit of total volume of the porous electrode; this specific surface area is designated by a_e. The geometrical methods, as for example the filamentary analog [18], do not apply to foams, principally owing to the fact that the geometry of the sides of the skeleton is not well defined. Physical methods seem to be more appropriate. Among these physical methods, two were applied: (i) a static method involving gaseous adsorption (BET method) using krypton; (ii) a dynamic method based on the measurement of the static pressure drop of a liquid flowing through the porous medium in forced flow. Such a method simulates the use of the porous medium as a flow-by porous electrode and permits study of the hydrodynamic behaviour of the foam.

4.1. *Application of the BET method*

This method was previously applied for the materials considered in [9]. The specific surface area, $(a_e)_{BET}$ was deduced from the plot of the krypton adsorption isotherm on the foam at the temperature of liquid nitrogen (77.5°K). The details of the experimental procedure and the method of calculation of $(a_e)_{BET}$ are given in [19]. Table 3 gives the values of the adsorbed surface per gram of material, S, and those of $(a_e)_{BET}$; this specific surface area $(a_e)_{BET}$ is termed the *static* specific surface area, owing to the method used. The values deduced for $(a_e)_{BET}$ are between $20\,000\,m^2\,m^{-3}$ and $40\,000\,m^2\,m^{-3}$ and are much lower than the values of about $130\,000\,m^2\,m^{-3}$ which were given in [9] for other foams.

4.2. *Application of the pressure drop method*

4.2.1. Presentation of the method. The Ergun equation describes the static pressure drop for a liquid flowing through a porous medium [20–22]:

$$\frac{\Delta P}{H} = A\bar{u}^2 + B\bar{u} \qquad (3)$$

Table 3. Values deduced for a_e by the BET method

Foam	*Adsorbed surface per unit of weight of material* ($m^2\,g^{-1}$)	$(a_e)_{BET}$ ($m^2\,m^{-3}$)
G100	0.155	41 000
G60	0.125	30 000
G45	0.095	19 000

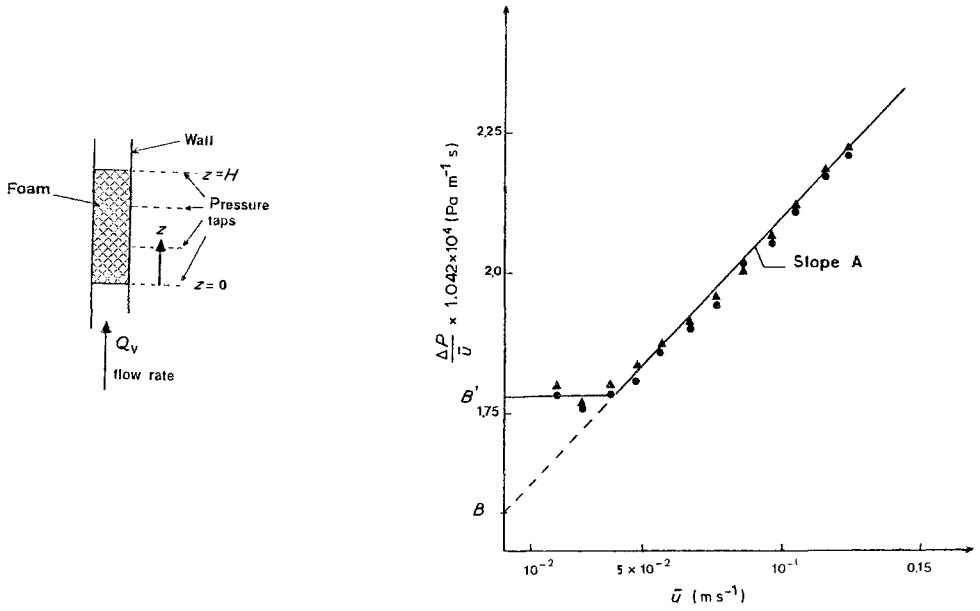

Fig. 4. Example of application of the Ergun equation to foam G100. Height of foam = 5.1 cm, distance between the pressure taps H = 4.5 cm.

where H is the height of the porous medium, $\bar{u}$ the mean liquid velocity in the empty container; A and B are factors which contain physical and geometrical parameters of the system. Expression 3 indicates that the pressure drop, ΔP, results from a laminar contribution (term $B\bar{u}$) and a turbulent contribution (term $A\bar{u}^2$). Coefficients A and B particularly contain the specific surface area per unit volume of solid, a_s (related to a_e by $a_e = a_s(1 - \bar{\varepsilon})$) and the mean overall tortuosity of the pores T; these two parameters obey the following expressions, respectively:

$$a_s = \left[\frac{B^3}{A^2}\frac{(0.096\varrho H)^2}{(2\gamma\mu H)^3}\frac{\bar{\varepsilon}^3}{(1-\bar{\varepsilon})^4}\right]^{1/4} \quad (4)$$

$$T = \left[\frac{A^2}{B}\frac{2\gamma\mu H}{(0.096\varrho H)^2}\bar{\varepsilon}^3\right]^{1/4} \quad (5)$$

In these expressions ϱ is the liquid density, μ the dynamic viscosity of the liquid and γ the circularity factor of the pores. The literature suggests that the value of γ is generally between 1 and 1.5 for various geometrical sections of the pores, with the value 1.25 as an approximation [22]. *A priori* the value of 1.25 was taken here for γ but such a choice has only a small influence on the calculation of a_S and T from expressions 4 and 5.

The static pressure drop, ΔP, was measured for various heights H (varying between 2.5 and 10.5 cm) of the three foams, according to the schematic representation of Fig. 4; the liquid is flowing perpendicularly to the smaller cross-sectional area of the foam sheet. In the experiments the foam is located in a rectangular channel; the foam defines the thickness of this channel. Such a positioning of the foam with respect to the liquid flow direction is the same as that encountered in the flow-by porous electrodes constructed with this material [10, 11]. The liquid used in the pressure drop determinations is the same as the electrolyte used in the mass transfer studies [10]; from the point of view of the hydrodynamics, the determinant component of this liquid is NaOH 1 N. The experiments were made at 30° C; at this temperature the dynamic viscosity is $\mu = 1.07 \times 10^{-3}\,\mathrm{kg\,m^{-1}\,s^{-1}}$ and the density is $\varrho = 1.07 \times 10^{3}\,\mathrm{kg\,m^{-3}}$. The mean liquid velocity, $\bar{u}$, in the empty channel was varied between 0.01 and 0.15 m s^{-1}.

Further pressure drop measurements were made on stacks of foam placed in a cylindrical column. These experiments were undertaken in order to explain mass transfer results in flow-through porous electrodes and will be commented on in [11].

4.2.2. Results. According to the Ergun equation, the plot of the values of $\Delta P/(H\bar{u})$ vs $\bar{u}$ leads to a straight line; an example of results is given in Fig. 4. The values of the slope A and of the initial ordinate B of this straight line allowed the calculation of a_s and T from Equations 4 and 5. For foams G60 and G100 — as is the case in Fig. 4 — a horizontal plateau, $\Delta P/(H\bar{u}) = B'$, appears at small $\bar{u}$ values for small heights H. Such a plateau may reveal that the corresponding porous media flow resistance is mainly due to the viscous friction; it suggests the existence of an entrance region for the establishment of the inertial flow regime within the foam. However B and B' can be considered as equal owing to the scatter in the values of B for various heights of a given foam.

The mean arithmetical values, $\bar{A}$ and $\bar{B}$, of A and B

Table 4. Values of A and B obtained from the pressure drop measurements

Foam	$\bar{A}$ ($Pa m^{-3} s^2$)	$\bar{B}$ ($Pa m^{-2} s$)	$\bar{B}/\bar{A}$ ($m s^{-1}$)
G100	16.2×10^5	3.4×10^5	0.21
G60	9.8×10^5	1.3×10^5	0.13
G45	6.2×10^5	5×10^4	0.08

Table 5. Values of the parameters deduced by the application of the Ergun equation

Foam	a_s (m^{-1})	$(a_e)_{Ergun}$ (m^{-1})	R_h (m)	$(\bar{d}_p)_{Ergun}$ (m)	T
G100	$(3.7 \pm 0.4) \times 10^5$	$(9.25 \pm 1) \times 10^3$	1.05×10^{-4}	4×10^{-4}	1.15 ± 0.10
G60	$(2.3 \pm 0.3) \times 10^5$	$(5.75 \pm 0.75) \times 10^3$	1.7×10^{-4}	7×10^{-4}	1.15 ± 0.10
G45	$(1.4 \pm 0.35) \times 10^5$	$(3.5 \pm 0.9) \times 10^3$	2.8×10^{-4}	1.1×10^{-3}	1.20 ± 0.15

are tabulated in Table 4, together with the values of $\bar{B}/\bar{A}$. This ratio $\bar{B}/\bar{A}$ has the dimension of velocity and represents the velocity $\bar{u}$ for which the viscous and the inertial contributions are equal. This transition velocity $\bar{B}/\bar{A}$ decreases when the mean pore diameter increases (foam G100 to foam G45). For $\bar{u}$ smaller than $0.005\ m\ s^{-1}$, only the laminar contribution prevails. The ratio μ/B is the permeability of the foam, as defined in Darcy's law.

Table 5 gives the values deduced for a_s and T using Equations 4 and 5, respectively, and also for the following parameters: (i) $a_e = a_s(1 - \bar{\varepsilon})$, called $(a_e)_{Ergun}$, and which is *dynamic* specific surface area; (ii) the hydraulic pore radius $R_h = \bar{\varepsilon}/(a_e)_{Ergun}$; (iii) the mean pore diameter $\bar{d}_p = 4R_h$.

5. Discussion of the results

The tortuosity, T, has nearly the same value (between 1.15 and 1.20) for the three foams and the specific surface area $(a_e)_{Ergun}$ is approximately 5 times smaller than $(a_e)_{BET}$. Such a difference is not surprising, in view of the methods used [15, 17]. As a rough approximation, if one considers that the openings between two adjacent alveolar cavities are toroidal, it can be shown that the developed surface of such a torus would be between 3 and 8 times higher than the projected surface on the plane of the torus.

Concerning the application of the nickel foams as flow-through or flow-by porous electrodes, the following remarks may be made: (i) the specific surface area $(a_e)_{Ergun}$ has to be considered for the characterization of the liquid flow within the structure, and thus the characteristic dimension of this structure would be the hydrodynamic pore diameter; (ii) for the electrochemical aspect, the true available specific surface area is between $(a_e)_{Ergun}$ and $(a_e)_{BET}$, but probably far from $(a_e)_{BET}$, even for materials without microporosity or internal porosity. The problem is that this available electrochemical surface area cannot be known with certainty.

The mass transfer data will be presented in [10] in the form of the product $\bar{k}_d a_e$ of the mass transfer coefficient $\bar{k}_d$ and the specific surface area. This product $\bar{k}_d a_e$ has the dimension of s^{-1} and is a parameter sufficient for design calculations.

The mean pore diameter $(\bar{d}_p)_{micro}$, deduced from optical microscopy, principally involves small pores, i.e. the openings between two adjacent alveoli. This probably explains why this diameter is about 2 times smaller than the mean pore diameter deduced by applying the Ergun equation to the whole pores.

Figure 5 gives, as function of the grade value, the variations of $1/(\bar{d}_p)_{micro}$ and $1/(\bar{d}_p)_{Ergun}$, and also the variations of $(a_e)_{BET}$ and $(a_e)_{Ergun}$. Although only three foams were considered in the present work, it may be seen that each of the four above parameters is proportional to the grade.

Table 6 compares values of the specific surface area of several materials considered for the construction of porous electrodes, with indications of the method of determination used. The following observations may be made.

(i) The specific surface area indicated by the manufacturer for a given grade of RVC [6] is comparable to that deduced from the Ergun equation for nickel foam of the same grade.

(ii) The values of a_e used in [1] were determined by

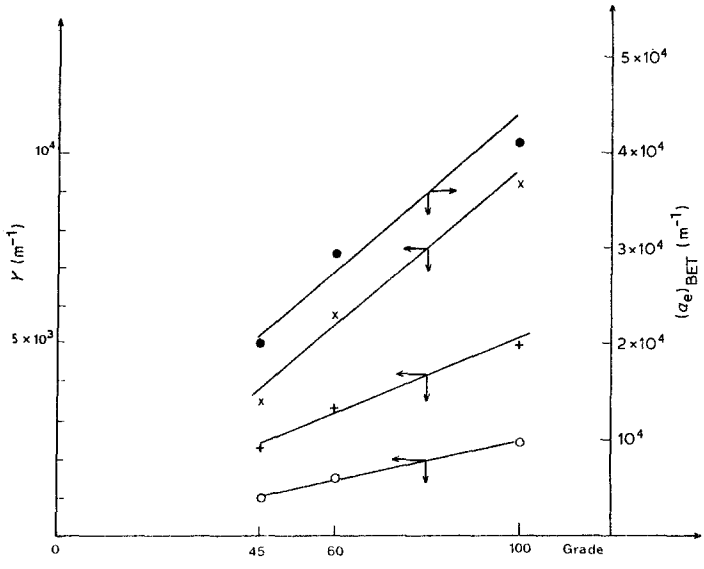

Fig. 5. Variations of $1/\bar{d}_p$ and a_e with foam grade. ●, $(a_e)_{BET}$; x, $(a_e)_{Ergun}$; +, $1/(\bar{d}_p)_{micro}$; ○, $1/(\bar{d}_p)_{Ergun}$.

Table 6. Comparison of the values of a_e obtained for different materials by various methods

Material	*Type*	a_e $(m^2 m^{-3})$	*Method*	*Reference*
Ni foam	Grade 100	9000–40 000	Ergun–BET	Present work
Ni foam	Grade 60	6000–30 000	Ergun–BET	Present work
Ni foam	Grade 45	3500–10 000	Ergun–BET	Present work
RVC foam	Grade 100 (100 ppi)	6600	Unknown	[6, 14, 7]
RVC foam	Grade 60 (60 ppi)	2500	Unknown	[6]
Cu foam	Grade 60 (60 ppi)	2500	Coulometry	[1]
Ni microporous membrane		600 000	Gas permeametry	[15]
Ni felt		500 000	BET	[9]
Expanded metal		500–10 000	Geometrical	[23]
Fixed bed of spheres	Particle diameter $\bar{d}_p$ 0.2–1 mm	2200–10 000	$a_e = \frac{6(1-\bar{\varepsilon})}{\bar{d}_p}$	

coulometry; the method gave, for the foam of grade (or ppi) 60, a specific surface area nearly 2.5 times smaller than for a nickel foam of the same grade, as determined using the Ergun equation.

(iii) Microporous membranes present very high specific surface areas which are comparable to the areas measured for nickel felts by means of the BET method [9]. However, the analysis of experimental mass transfer results obtained with such microporous membranes [15] shows that the whole surface is not all used, probably owing to capillary phenomena.

(iv) With regards to nickel felts, the high value of $(a_e)_{BET}$ is due to the internal porosity of the fibres. Such a high surface is not available for an electrochemical application; on the contrary, it could induce difficulties in eventual applications.

Thus, the value measured for a_e depends greatly on the method used; in view of the application of the porous materials as flow-through or flow-by electrodes, it is realistic to measure a_e preferably by a dynamic method, in conditions analogous to the true conditions of use.

Finally, it is useful to state again how relatively easy it is to construct porous electrodes with metallic foams. As previously indicated in [9], the material can be squashed, thus facilitating the feeding of the current to the foam and the construction of a stack of foams. Also the fact that other electrochemically interesting metals (silver, gold, lead, etc.) could be fabricated as foams is a favourable aspect towards a growing interest in the industrial electrochemical application of flow-by porous electrodes made of metallic foams.

6. Conclusions

Nickel foams were characterized by different methods. The empirical relation between the grade and the pore diameter was established. The specific surface area was deduced using two methods leading to values which differed by a factor of 5. Thus, the true available electrochemical specific surface area cannot be known with certainty.

The foams studied have a similar texture, which is undoubtedly a consequence of the initial inert structure used in the fabrication process.

Owing to the parameters which influence the effectiveness of porous electrodes [23, 24], there is no doubt that metallic foams are potentially interesting for electrolytic industrial processes needing high conversion per pass, due to their high porosity, small electrical resistivity and high specific surface area.

Acknowledgements

The authors thank the Direction des Etudes et Recherches d'Electricité de France for its financial support during this work and the Society SORAPEC for the free supply of the materials.

References

[1] A. Tentorio and U. Casolo-Ginelli, *J. Appl. Electrochem.* **8** (1978) 195.
[2] D. A. Cox, PhD Thesis, University of Southampton (1981).
[3] M. Fleischmann and R. E. W. Jansson, *Electrochim. Acta* **27** (1982) 1023.
[4] M. Fleischmann and R. E. W. Jansson, *Electrochim. Acta* **27** (1982) 1034.
[5] J. Chaussard, R. Rouget and M. Tassin, *J. Appl. Electrochem.* **16** (1986) 803.
[6] The Electrosynthesis Co., PO Box 16, East Amherst, New York 14051, USA.
[7] M. Matlosz and J. Newman, *J. Electrochem. Soc.* **133** (1986) 1850.
[8] Société SORAPEC, 192, rue Carnot, 94120 Fontenay Sous Bois, France.
[9] J. M. Marracino, F. Coeuret and S. Langlois, *Electrochim. Acta* **32** (1987) 1303.
[10] S. Langlois and F. Coeuret, *J. Appl. Electrochem.* **19** (1988) 51.
[11] S. Langlois and F. Coeuret, *J. Appl. Electrochem.* (to be submitted).
[12] J. Jorne and E. Roayaie, *J. Electrochem. Soc.* **133** (1986) 1649.
[13] R. Alkire, B. Gracon, T. Grueter, J. Marek and P. Blackburn, *J. Electrochem. Soc.* **127** (1980) 1085.
[14] J. Wang, *Electrochim. Acta* **26** (1981) 1721.
[15] S. M. Mohnot and E. L. Cussler, *Chem. Eng. Sci.* **39** (1984) 569.
[16] T. C. Van Vechten, D. S. Lashmore, C. E. Johnson and J. C. Puippe, *Plating Surf. Finish.* **73** (1986) 45.

[17] F. Rouquerol, 'Texture des solides poreux ou divisés', Techniques de l'Ingénieur, Paris (1968) P3645.
[18] T. Katan and H. F. Bauman, *J. Electrochem. Soc.* **122** (1975) 77.
[19] S. Langlois, Thesis, Université de Rennes 1, June (1988).
[20] I. F. MacDonald, M. S. El Sayed, K. Mow and F. A. Dullien, *Inq. Eng. Chem. Fund.* **18** (1979) 199.
[21] C. W. Crawford and O. A. Plumb, *J. Fluids Engng* **108** (1986) 343.
[22] D. Pech, Thèse de Doctorat de 3ème cycle, I.N.P. de Grenoble, France (1984).
[23] F. Coeuret and A. Storck, Eléments de Génie Electrochimique, Tec. Doc., Lavoisier, Paris (1984).
[24] Y. Volkman, *Electrochim. Acta* **24** (1979) 1145.